THE JOURNAL OF PHYSICAL CHEMISTRY C

Article

Cite This: J. Phys. Chem. C 2018, 122, 20817−20826

pubs.acs.org/JPCC

Adsorption of Surfactants on α-Fe_2O_3(0001): A Density Functional Theory Study

Chiara Gattinoni,*[,†,‡] James P. Ewen,[‡] and Daniele Dini[‡]

[†]Department of Materials, ETH Zürich, Zürich 8092, Switzerland

[‡]Department of Mechanical Engineering, Imperial College London, London SW 72AZ, United Kingdom

Supporting Information

ABSTRACT: From corrosion inhibition to lubrication, a detailed understanding of the interactions between surfactants and iron oxide surfaces is critical for a range of industrial applications. However, there is still limited understanding of this behavior at the atomic-level, which hinders the design of improved surfactant molecules. In this study, the adsorption of three surfactants which are commonly employed as lubricant additives (carboxylic acid, amide, monoglyceride) on a α-Fe_2O_3(0001) surface is studied with density functional theory. The nature and strength of the adsorption for the different surfactants, as well as their propensity to deprotonate on the surface, is studied at a range of surface coverages. In agreement with the available experiments, strong chemisorption on α-Fe_2O_3(0001) is observed for all cases considered. Dissociation is energetically favorable for carboxylic acid and glyceride surfactants through the formation of a surface hydroxyl group, whereas this is not the case for amides. Glycerides form the most strongly adsorbed films at both low and high surface coverage due to the presence of multiple functional groups, which can all act as binding sites. However, the large size of the glyceride headgroup also means that adsorption is stronger at low coverage, where the formation of multiple bonds with the surface is possible, than at high coverage. Conversely, carboxylic acid films have similar stability at low and high coverage, where van der Waals forces between proximal tailgroups stabilize the adsorption structures. The results of this study provide atomic-level insights which help to explain friction results from previous macroscopic tribology experiments and classical molecular dynamics simulations. They also facilitate the molecular design of new surfactants to maximize the adsorption energy, surface coverage, and ultimately friction reduction on iron oxide surfaces.

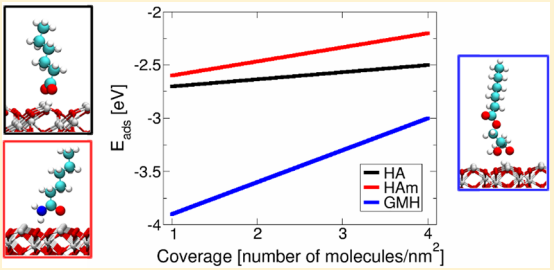

INTRODUCTION

Understanding the nature and strength of surfactant adsorption on iron oxide surfaces is important for a range of applications, from stabilizing iron oxide nanoparticles for use as biomarkers and catalysts[1] to extracting iron ore for steel production[2] and to protecting surfaces for corrosion inhibition.[3] Another prominent application, especially with growing concerns regarding CO_2 emissions, is as friction modifiers,[4] which are lubricant additives that reduce friction and wear in machine components and thus increase the energy efficiency of engineering systems.[5]

Within this class of additives, organic friction modifiers (OFMs) are prominent because they are based solely on C, H, O, and N atoms and are not environmentally harmful. OFMs are amphiphilic surfactant molecules that contain nonpolar aliphatic tailgroups attached to polar headgroups.[4] They adsorb to metal, ceramic, or carbon-based surfaces[6] through their polar headgroups, eventually forming high coverage monolayers.[4] These monolayers can prevent the direct contact of opposing sliding surfaces due to van der Waals (vdW) forces between proximal nonpolar tailgroups.[4] Several headgroups have been industrially considered; however, significant improvements have been hindered by a lack of atomic-level understanding regarding their adsorption behavior. Carboxylic acid headgroups are the most widely studied; however, due to their corrosive nature, they are no longer commercially attractive.[4] On the other hand, noncorrosive amide and glyceride OFMs are more industrially relevant, and the latter has also been shown to give lower friction than carboxylic acids in macroscopic tribology experiments.[7]

The majority of engine components are made from steel, which forms iron oxide surfaces when exposed to air.[8] Therefore, OFM film formation on iron oxide surfaces has attracted significant research interest.[4] Some structural information has been obtained from experimental techniques such as the quartz crystal microbalance,[9] sum frequency generation vibrational spectroscopy,[10] polarized neutron reflectometry,[11,12] the surface force apparatus,[13] and in situ atomic force microscopy.[14,15] These methods can be used to monitor monolayer formation and gather information such as film thickness and molecular tilt angle. However, they provide no information regarding the surface chemistry, i.e., the nature and strength of the interaction between OFM molecules and the surface. For the rational design of more effective OFM

Received: June 20, 2018
Revised: August 17, 2018
Published: August 21, 2018

DOI: 10.1021/acs.jpcc.8b05899
J. Phys. Chem. C 2018, 122, 20817−20826

molecules, an atomic-level understanding of the adsorption process is critical. X-ray photoelectron spectroscopy (XPS) and in situ Fourier-transform infrared (FTIR) spectroscopy studies of carboxylic acids OFMs on steel surfaces have given some insights in this regard. For example, early XPS studies[16] suggested that stearic acid (SA) films were only physisorbed on steel surfaces. However, more recent XPS and polarization modulation-infrared reflection absorption spectroscopy (PM-IRRAS) analysis suggested that chemisorption also occurs for SA.[17]

Molecular modeling studies have also provided insights into the nanoscale structure of OFM films on iron oxide surfaces.[18] For example, classical nonequilibrium molecular dynamics (NEMD) simulations of OFM monolayers have shown how the film structure of carboxylic acid, amide, and glyceride OFMs affects their friction response.[19−22] Amide and particularly glyceride OFMs were more effective at reducing friction than carboxylic acid OFMs at all coverages,[20] in agreement with experiment.[7] However, classical MD simulations are based on empirical force-fields which are generally not able to investigate chemical reactivity,[18] and so alternative methods are required to accurately determine the nature and strength of OFM adsorption on iron oxide surfaces.

Quantum mechanical (ab initio) calculations, particularly density functional theory (DFT), have been used extensively over the last few decades to investigate a large variety of problems in condensed matter physics, biology, catalysis, and elsewhere.[23] In recent years, significant interest has arisen in applying this method to study the reactivity of lubricant additives on solid surfaces.[24−30] Due to its relatively large computational cost, DFT is generally limited to static calculations. However, ab initio NEMD simulations investigating the reactivity of lubricant additives subjected to pressure and shear between iron surfaces have recently been reported.[31] Less computationally intensive ab initio calculations of OFM adsorption on iron oxide surfaces using the tight-binding (TB) approximation[32] have also been performed.[33] They suggested that that carboxylic acids mostly chemisorb on iron oxide surfaces, regardless of the tailgroup molecular structure.[33] Coupled techniques, such as quantum chemical tight-binding coupled with classical molecular dynamics (TB/MD),[17] have also been used to study adsorption of OFMs on iron oxide surfaces dynamically.[17,34] One of these studies suggested that, although carboxylic acid molecules chemisorb on iron oxide surfaces when present at high surface coverage, they only physisorb at lower coverage.[34] Further TB/MD simulations suggested that, while carboxylic acids mostly chemisorb on iron oxide surfaces and fully chemisorb on nascent iron surfaces, they mostly physisorb on iron hydroxide surfaces.[34] There are notable differences between the TB/MD results, which suggest that the carboxylic acid molecules remain intact when adsorbed, and XPS and PM-IRRAS experiments, which suggest dissociation to form a carboxylate.[17] To the authors' knowledge, no ab initio investigations of adsorption of the more commercially relevant amide or glyceride surfactants on iron oxide surfaces have been reported in the literature.

In this study, the nature and strength of adsorption of three different surfactants on an iron oxide surface will be investigated using DFT. More specifically, the adsorption energy and dissociation behavior of carboxylic acid, amide, and glyceride OFMs on a α-Fe_2O_3(0001) surface will be determined. The DFT calculations performed in the present study highlight important differences between the headgroup chemistries and surface coverages. The insights provided by this study help to explain macroscopic tribology experiments and provide useful information for the molecular design of more effective OFM additives.

METHODS

Density functional theory (DFT) was employed throughout this study using VASP[35−37] with the projector augmented wave (PAW) method[38] and spin polarization. The optB86b-vdW functional[39] has been employed. This is a nonlocal correlation functional which includes vdW interactions and has been shown to perform well on a large number of problems of molecular adsorption.[26,40−45] The plane-wave expansion was cutoff at 550 eV and for bulk α-Fe_2O_3 (hematite) a Monkhorst−Pack k-points mesh of 4 × 4 × 2 was used for the hexagonal unit cell. A dipole correction[46,47] was added in all cases.

Surfactant Molecules. The tailgroups in commercial OFMs are generally unbranched, aliphatic chains containing 12−20 carbon atoms. This is mainly because they are readily available from natural fats and oils, are soluble in most base oils, and effectively reduce friction and wear.[4] Using molecules of this size would be prohibitively computationally expensive given the large number of DFT calculations performed in this study. Since the focus here is the interaction of the headgroups with the surface, the saturated tailgroups are the minimum length to ensure that the geometry and partial charges within the headgroups are representative of longer tails. Tests show that C_6 groups are sufficient to achieve this, as shown in the Supporting Information (SI). Moreover, previous DFT calculations have shown that the structural and electronic character of carboxylic acid headgroups are insensitive to tailgroup length,[48] while TB calculations have suggested that the headgroup-surface interaction strength is similar, regardless of tailgroup molecular structure.[33] Therefore, hexanoic acid (HA), hexanamide (HAm), and glycerol monohexanate (GMH) surfactants are used in this study (see Figure 1a).

Further tests were performed to ensure that vdW interactions between tailgroups in neighboring molecules were adequately described by the optB86b-vdW functional.

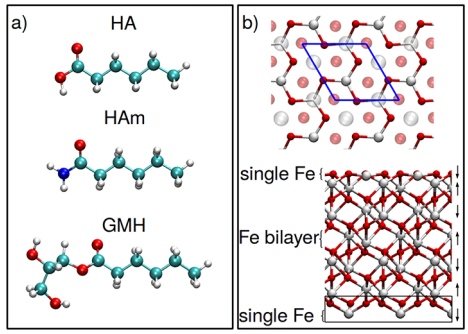

Figure 1. (a) Three surfactant molecules considered in this study: HA (top), HAm (middle), and GMH (bottom). O is shown in red, N in blue, H in white, and C in cyan. (b) Top (top) and side (bottom) view of the single Fe-terminated 15-layer slab used as a substrate for the adsorption calculations. O is shown in red and Fe in gray. In the top view, the top layer is shown with solid atoms for clarity, the layer below with transparent atoms. The blue box (top panel) indicates the unit cell and periodic images are shown. In the side view (bottom panel), the black box shows the layers which are kept fixed, the arrows show the direction of the magnetic moment for every Fe bilayer.

DOI: 10.1021/acs.jpcc.8b05899
J. Phys. Chem. C 2018, 122, 20817−20826

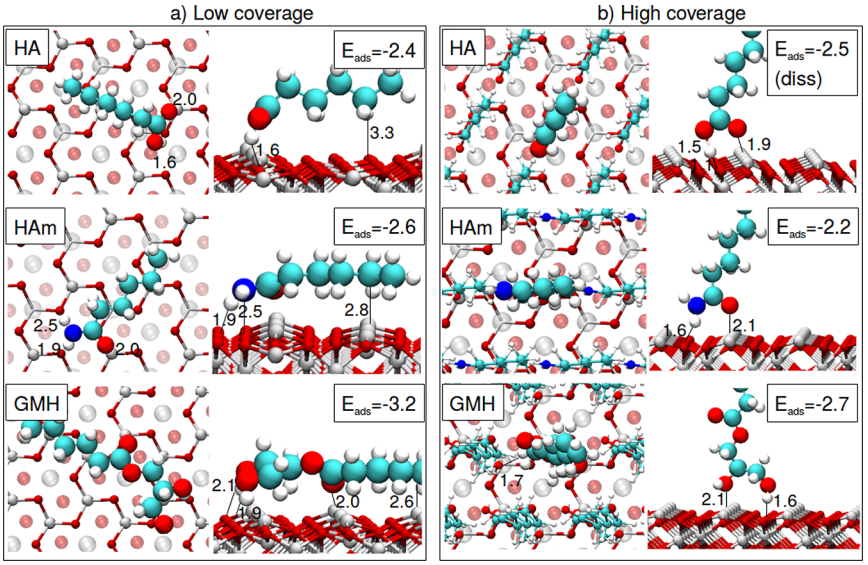

Figure 2. Top and side view of the most stable intact adsorbed structures at (a) low and (b) high coverage for HA, HAm and GMH. Fe atoms are shown in gray, O in red, H in white, C in cyan, and N in blue. E_{ads} shown in eV. In the top view, OFM periodic replicas are shown as smaller atoms. In the side view, the periodic images are not shown for clarity. Please note that the high coverage structure for HA is deprotonated since no stable intact structure was found.

Due to the lack of experimental and quantum chemical data for HA, HAm and GMH, well-studied pentane molecules were used as a model for the tailgroups. It was confirmed that the interaction energy between two pentane molecules was correctly described within 3% of the MP2-calculated value[49−51] with the optB86b-vdW functional (details in the SI).

***α*-Fe_2O_3(0001) Slab.** For the iron oxide substrate, *α*-Fe_2O_3 was used since it is the most thermodynamically stable form[52] and is a common steel corrosion product.[8] A Hubbard $U-J = 4$ eV (in the Dudarev approach[53]) was added to account for electronic correlations in the Fe 3d orbitals. This correction leads to a band gap of 1.98 eV, which is within the experimentally observed range (1.9−2.2 eV).[54,55] Moreover, good agreement with previous DFT and experimental results for the lattice parameters[56] and magnetic moments[57−61] was obtained (see details in the SI).

The *α*-Fe_2O_3(0001) surface presents itself as a stacking of an O layer followed by an iron bilayer, as shown in Figure 1b. Each Fe bilayer is ferromagnetic and neighboring bilayers are antiferromagnetically coupled.[56] Slabs of 15 atomic layers terminated by a single Fe layer were employed for the adsorption calculations (Figure 1b). The single Fe-terminated structure has been shown by numerous theoretical and experimental studies to be the most stable at room temperature.[52] Good agreement with previous DFT studies was found for the values of the surface energy and the degree of relaxation of the surface layer (details in the SI).[59,62,63] Fe adatoms have been used in a subset of the calculations to provide stability to the adsorbed complexes;[26] these are clearly indicated in the text.

Periodic boundary conditions are employed in the in-plane directions[47] while a vacuum of 15 Å in the out-of-plane direction was added to prevent interactions between neighboring cells. One surfactant molecule was included in 2 × 2 and 1 × 1 cells for respectively the low coverage (~1 nm^{-2}) and high coverage (~4 nm^{-2}) calculations. These surface coverages are similar to those in previous experimental[12] and molecular modeling[20] studies. In all cases, the bottom three hematite layers (see Figure 1b) were kept fixed to simulate bulk conditions.

Adsorption Energies. Adsorption energies (E_{ads}) were calculated as

$$E_{ads} = (E_{sys} - E_{slab} - N_{mol} \times E_{mol})/N_{mol} \quad (1)$$

where E_{sys} is the total energy of the adsorbed complex, E_{slab} is the total energy of the substrate (an *α*-Fe_2O_3(0001) slab which might contain Fe adatoms), E_{mol} is the total energy of the gas-phase molecule, and N_{mol} is the number of molecules in each cell. A negative value of E_{ads} indicates a stable adsorbed structure. In a subset of systems, which are clearly indicated in the text, an additional Fe surface atom was added to stabilize the adsorbed structures.[26] In this case, it is necessary to compare the energies of systems containing a different number of atoms. Therefore, free energies of adsorption have been calculated as a function of the oxygen chemical potential, using the ab initio thermodynamics formalism.[64,65] The free energy of adsorption, ΔG, for the limits of low (ΔG^{low}) and high (ΔG^{high}) O partial pressures is expressed as

$$\Delta G^{low} = \frac{1}{A}(E_{sys} - E_{slab}^{single} - N_{mol}E_{mol} - \Delta N_{Fe}E_{Fe}) \quad (2)$$

$$\Delta G^{high} = \Delta G^{low} - \frac{\Delta N_{Fe}}{2A}\Delta G_{form} \quad (3)$$

where ΔG_{form} is the formation energy of hematite, E_{slab}^{single} is the total energy of a single-Fe terminated *α*-Fe_2O_3(0001) slab (without Fe adatoms), ΔN_{Fe} is the number of Fe adatoms, and E_{Fe} is the total energy of a single Fe atom in the iron bcc bulk. Further details of the derivation[59,65] are shown in the SI.

RESULTS AND DISCUSSION

In this section, results of the DFT calculations investigating the adsorption behavior of HA, HAm, and GMH molecules on *α*-Fe_2O_3(0001) are presented and discussed. The adsorption of intact molecules at low and high coverage is examined first, to

DOI: 10.1021/acs.jpcc.8b05899
J. Phys. Chem. C 2018, 122, 20817−20826

understand the interaction of the different headgroups with the surface. Investigations of the dissociation process and the influence of environmental conditions such as temperature and pressure on this process are then presented. Finally, a comparison to previous experimental and modeling studies and implications for the molecular design of improved friction modifiers is discussed.

Adsorption Structures and Coverage Dependence. The most stable adsorption structures for HA, HAm, and GMH (both intact and deprotonated) on α-Fe_2O_3(0001) at low (~1 mol/nm^2) and high (~4 mol/nm^2) coverage were established by geometry optimization of at least ten initial configurations per system (with different molecule, coverage, and protonation state). Figure 2 shows the most stable intact adsorption structures at low (a) and high (b) coverage for the three surfactant types. For all of the molecules, the most stable intact adsorption structures maximize both the number of bonds between the headgroup and the surface, as well as the vdW interactions between the tailgroups and the surface (at low coverage) or between neighboring tailgroups (at high coverage).

This implies that, at low coverage, the adsorption structures with the surfactants lying almost flat to the surface (shown in Figure 2a) are always more stable than structures with the tailgroups perpendicular to the surface (shown in Figure S4). This is confirmed by the adsorption energies for the most stable low coverage structures in these flat (E_{ads}^{flat}) and upright (E_{ads}^{up}) conformations (Table 1). Flat-lying molecules are preferred at low coverage for all the surfactants (in all cases $E_{ads}^{flat} < E_{ads}^{up}$), with the tailgroup-surface vdW interactions stabilizing the adsorbed complexes by 0.2−1.4 eV depending on the molecule.

Table 1. Adsorption Energies Calculated with eq 1 for Flat (Shown in Figure 2) and Upright (Shown in Figure S4) Low Coverage Structures of the Three Surfactants Considered in This Study[a]

low coverage structure	E_{ads}^{up}	E_{ads}^{flat}
HA	−2.15	−2.37
HAm	−2.12	−2.62
GMH	−2.63	−3.19

[a]Energies are in eV.

In all cases, the tailgroup C atoms remain in an "all-trans" conformation. For the most stable flat-lying systems in Figure 2a, the tailgroups are orientated with C atoms either equidistant to the surface (e.g., HAm and GMH) or at high-low positions with respect to it (e.g., HA). The preferred conformation depends on the geometry of the headgroup which, due to its stronger interactions with the surface, ultimately determines the overall orientation of the molecule on the surface. For HA, the minimum C−Fe distance is approximately 3.3 Å, suggesting that only physisorption between the surface and the tailgroup occurs. This postulation is confirmed in Figure 3 which shows that minimal charge transfer between the surface and the tailgroup occurs. It is noteworthy that adsorbed HA structures with all of the C atoms equidistant to the surface were also observed in our calculations; however, they spontaneously deprotonated and are not stable as intact structures. They will thus be discussed in the next section.

As shown in Figure 2a, the intact HA headgroup forms two bonds with the surface; O−Fe bond through the carbonyl O and one H−O_{surf} bond (where O_{surf} is an O atom belonging to the hematite slab). At low coverage, intact HAm forms three bonds with the substrate via its headgroup; two H−O_{surf} bonds and one O−Fe bond through the carbonyl O (Figure 2a). Figure 2a shows that the two H atoms bonded to the N atom are at rather different distances from the O_{surf} atoms, suggesting that only one of them forms a strong bond with the surface. The headgroup geometry allows the tailgroup C atoms to be equidistant from the surface (C−Fe distance ~2.8 Å). This arrangement of the C atoms leads to stronger molecule−surface bonding through the tailgroup and a surface Fe atom is pulled outward by 0.8 Å from its relaxed position to maximize these interactions, with some charge transfer occurring (see HAm in Figure 3).

GMH also forms two H−O_{surf} bonds with the surface as well as one O−Fe bond through the carbonyl O. A number of isoenergetic configurations have been observed for GMH, with small differences between the rotation of the tail-group and the binding sites for the headgroup. This is unsurprising considering the complexity of the headgroup and the flexibility of the molecule, which can rearrange itself in multiple ways on the surface. A representative structure is shown in Figure 2a. Similar to HAm, the C atoms in the tailgroup are equidistant to the surface (C−Fe distance ≈2.6 Å), a surface Fe atom is pulled outward from its relaxed position, and some charge transfer between the surface and the tailgroup atoms occurs (see GMH in Figure 3).

The bond lengths for the headgroup-surface interactions at low coverage are shown in Figure 2a and they are generally ~1.6−2.5 Å. This suggests that all of the surfactants chemisorb on the surface, as confirmed through electron density difference plots (Figure 3) showing a significant amount of charge transfer between the headgroups and the surface. At low coverage, HA is the weakest-binding intact molecule (see

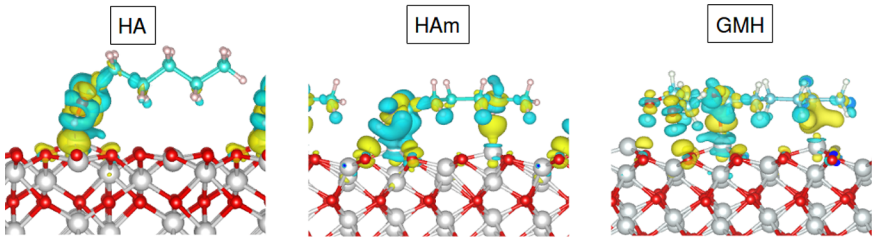

Figure 3. Electron density difference plots for the most stable low coverage structures for HA, HAm, and GMH. Green represents regions of charge density depletion, while yellow represents regions of accumulation. The isosurface level is 0.002 e/a_0^3 (where a_0 is the Bohr radius) for all structures.

DOI: 10.1021/acs.jpcc.8b05899
J. Phys. Chem. C 2018, 122, 20817−20826

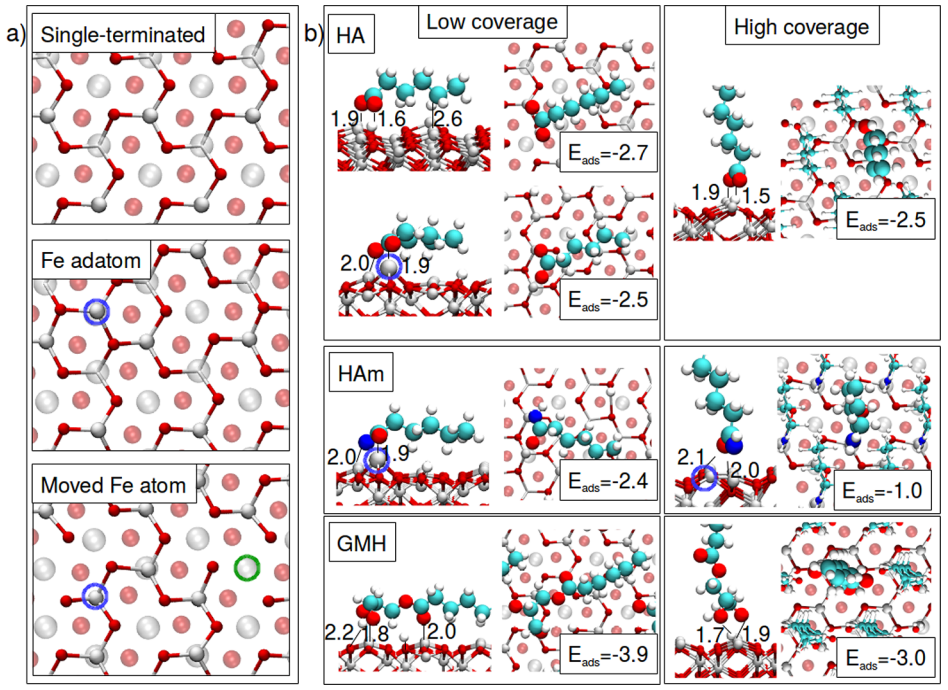

Figure 4. (a) Top views of the single-terminated surface (top), surface with adatom (middle, adatom circled in blue), and single terminated with an Fe surface atom moved from the most stable position (vacancy shown in green) to a "top layer" position (bottom, adatom circled in blue). (b) Most stable dissociated structures for the three surfactants at low and high coverage. The Fe adatom is circled in blue. O atoms are red, Fe in gray, H in white, N in blue, and C in cyan. Adsorption energies (E_{ads}) are reported in eV.

Table 1, E_{ads}^{flat}), since it only forms two bonds with the surface. Although intact HAm forms three bonds with the surface, only one of the H−O_{surf} bonds is strong because of both H atoms are bonded to the same N atom, making it impossible for both to be positioned close to O_{surf} atoms simultaneously. GMH is by far the strongest-binding intact molecule at low coverage. Similarly to HAm, it forms three headgroup-surface bonds, but they are from separate functional groups and the ester group is flexible, meaning that GMH orientates itself such that both alcohol H atoms can strongly bond to the surface.

For all three surfactants, the absolute value of the adsorption energy is similar between the low (Figure 2a) and high (Figure 2b) coverage cases (within 0.5 eV), despite the molecular conformations being very different. Steric interactions between neighboring molecules increase with increasing surface coverage, forcing the tailgroups into a more upright position.[12] However, the reduction in tailgroup−surface interactions, which help to stabilize the flat-lying configurations at low coverage, is partially compensated for by increased tailgroup−tailgroup vdW interactions.[26] Even at high coverage, the surfactant tailgroups are not completely perpendicular to the surface, but tilt at approximately 15−25° from the surface normal, in good agreement with experimental data for palmitic acid (C_{16} tailgroup)[11] and TB/MD simulations for SA.[34]

The adsorption energy trends between the three surfactants is different at high coverage compared to at low coverage. GMH is still the strongest-binding of the three surfactants but is less stable at high than at low coverage by ∼0.5 eV. This is due to the large size of its headgroup; the separate binding sites span ∼5 Å in the optimal low coverage conformation (see Figure 2a), and there is insufficient surface area available for all three binding sites to form bonds with the surface at high coverage. Consequentially, only one H−O_{surf} bond forms with the surface at high coverage and the second is replaced by a weaker H-bond (d_{bond} = 1.7 Å) between neighboring GMH molecules (see Figure 2b).

At high coverage, when HAm is rotated upright, it loses one of the H−O_{surf} bonds with the surface, thus also leading to a less stable system than at low coverage. Similar to GMH, this is partially compensated for by H-bonds between neighboring molecules (d_{bond} = 2.1 Å), but the configuration is still ∼0.4 eV less strongly bound than at low coverage. Intermolecular H-bonding in glyceride and amide films was also observed at high coverage in classical MD simulations.[20]

For HA, no stable intact high coverage structure was observed, since the system of closely packed upright HA molecules spontaneously dissociated in all of the calculations performed in this study. This reinforces what was observed for some of the low coverage systems, i.e., that HA spontaneously deprotonates when adsorbed on α-Fe_2O_3(0001). The dissociated structures are discussed in more detail in the following Section.

Dissociation upon Adsorption. The possibility of dissociation upon adsorption, where bonds between H atoms and electronegative headgroup atoms break, with the H atoms forming new bonds with O_{surf} atoms, was also considered. This can be expected to occur for some of the studied surfactants, particularly the carboxylic acid (HA), which can readily deprotonate to form a stable carboxylate.[33] Indeed, as shown in Figure 2b, HA spontaneously deprotonates at high coverage and no stable intact structure was observed. At high coverage, HA forms a H−O_{surf} bond (1.1 Å) with the surface, yielding a surface hydroxyl group. The O−H bond length within the adsorbed molecule (1.5 Å) increases significantly from the equilibrium distance for the intact molecule (1.05 Å), indicating that dissociation has occurred.

The high temperature and pressure conditions which OFMs operate under may also induce dissociation in otherwise stable

DOI: 10.1021/acs.jpcc.8b05899
J. Phys. Chem. C 2018, 122, 20817−20826

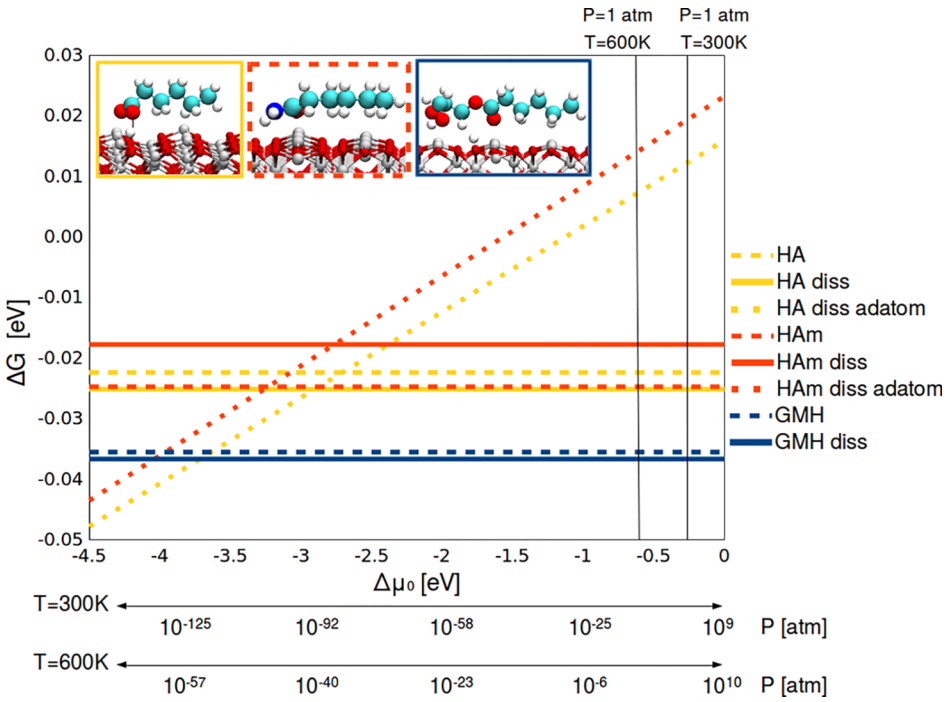

Figure 5. Gibb's free energies of adsorption for HA (yellow), HAm (red), and GMH (blue) at low coverage on α-Fe_2O_3(0001) as a function of the oxygen chemical potential, as calculated from eq 2 and 3. Dashed lines are for the most stable intact structure, solid lines for dissociated structures on a single Fe-terminated surface, and large-dotted lines for dissociated structures on a surface with an Fe adatom. No line corresponding to GMH dissociated structures with adatoms is present since these were not calculated. The most stable low coverage adsorption structure for each of the molecules is shown in the insets. The other intact and dissociated structures are shown in Figures 2 and 4, respectively.

systems.[17,34] In the following set of calculations, in addition to the most stable single Fe-terminated slab, some defective surface structures were also investigated. Many surface terminations have been studied for hematite, and some of these are more stable than the single Fe-termination under nonambient conditions of temperature and pressure.[66] Therefore, the possible addition of an extra surface Fe atom was also considered. Fe bilayers are present in bulk hematite (see the SI),[52] so the Fe adatom was positioned in one of the sites of the "missing" top Fe layer in the single-terminated surface (see Figure 4a, middle). In addition, the migration of a surface Fe from its most stable position to a "top layer" position was also studied (see Figure 4a, bottom). In both cases, the Fe adatom provides an extra adsorption site for the negatively charged O or N atoms in the deprotonated molecules which is expected to stabilize the adsorption structure.[26] The H atom remains in the simulation cell and is allowed to form a surface hydroxyl group. As for the intact structures shown in the previous section, a large number of dissociated configurations (at least ten per system) were optimized in order to account for different molecular orientations, H atom positions on the surface, and surface conditions. The results for the free energy of adsorption for the most stable structures of the three surfactants at low coverage are shown in Figure 5. The most stable dissociated structures at low and high coverage are shown in Figure 4. In Figures 5 and 4, Fe adatoms are highlighted with a blue circle.

In Figure 5, the yellow solid line is at lower energy than the dashed line, indicating that dissociation is thermodynamically favorable for HA at low coverage on the single-Fe terminated surface. The gain in adsorption energy for the structure shown in Figure 4b compared to the metastable intact structure in Figure 2a is ∼0.3 eV. At both HA coverages, the dissociated H atom, H_{diss}, forms a surface hydroxyl (H_{diss}−O_{surf}, with a bond length of ∼1.0 Å) and the deprotonated HA molecule forms a O−H_{diss} bond with this newly formed hydroxyl (see Figure 4b). Similar to the intact surfactants, flat-lying conformations are preferred at low coverage (see Table S2) and upright ones at high coverage (see Figure 4b). For dissociated HA at low coverage, another stable structure (E_{ads} = −2.5 eV) was identified by adding a Fe top layer atom and forming two O−Fe bonds instead (see Figure 4b). However, Figure 5 shows that this configuration (dotted yellow line) is less stable than the structure deprotonating on the single Fe-terminated surface (solid yellow line). It only becomes favorable at extremely low values of the O chemical potential (μ_O < 2.8 eV) which corresponds to very low O partial pressures or high temperatures, which are unlikely to occur in practical applications.

Unlike the other surfactants, dissociation for basic HAm is not thermodynamically favorable on the single-Fe terminated surface. This is shown in Figure 5 by the fact that the red solid line is at higher energy than the dashed line. Surprisingly, HAm can dissociate, although only at low coverage when stabilized by an Fe adatom. Similar to HA, deprotonation via an Fe adatom is only possible at extreme conditions of temperature or pressure (red dotted line in Figure 5). For example, at 300 K, the dissociated structure becomes stable at an oxygen partial pressure of $\sim 10^{-90}$ atm. At high coverage, the adsorption energy of the dissociated structure is always rather weak (∼−1.0 eV, Figure 4) and thus less stable than the intact structure.

Conversely, dissociation is always thermodynamically favorable for GMH on the single Fe-terminated surface; the blue solid line is at lower energy than the dashed line. On the single Fe-terminated surface, dissociation gives an energy

DOI: 10.1021/acs.jpcc.8b05899
J. Phys. Chem. C 2018, 122, 20817−20826

benefit of ∼0.7 eV at low coverage and ∼0.3 eV at high coverage (Figure 4b) compared to the most stable intact adsorption structures (Figure 2). Both alcohol groups in the glyceride can be deprotonated, but the most stable dissociated configuration at both coverages involves the deprotonation of only the primary alcohol group, with the secondary alcohol group remaining intact (Figure 4b). At both coverages, dissociation enables the formation a strong O−Fe bond (∼1.9 Å) between the dissociated alkoxy group and the surface. At low coverage, the carbonyl O in the ester group also forms a O−Fe bond, the intact secondary alcohol forms a H−O_{surf} bond, and the bridging ester O forms a H-bond with the newly formed surface hydroxyl, leading to a very stable adsorption structure (Figure 4b). The large headgroup size of GMH means that the molecule can rearrange itself such that the dissociated alkoxide group can bind to a nearby surface Fe atom. This obviates the need to include a Fe adatom to stabilize the adsorption structure, and thus defective hematite surfaces were not considered for GMH. An additional consideration for glycerides is the possibility of hydrolysis of the ester linkage.[22] However, when the C−O ester bond was broken in GMH, no stable adsorption structure on α-Fe_2O_3(0001) was observed, suggesting that water molecules are necessary for this to be possible even in the presence of a reactive surface.

In all cases, the migration of a Fe atom from a low-energy position to a less stable "top layer" position leads to systems which are more weakly adsorbed than the structures presented above (adsorption energies are found to be in the −1.0 to −2.0 eV range, structures not shown). Thus, adsorption structures on the single-Fe terminated surface are the most favorable for the majority of temperature and pressure conditions.

The energy trends between low and high coverage for the dissociated structures are similar as for the intact molecules. Dissociated HA shows similar adsorption energy at both coverages so, for a high concentration of adsorbants, a high coverage film can be expected to form. Conversely, dissociated GMH is adsorbed significantly more strongly at low coverage compared to high coverage. This suggests that the formation of high coverage films may not be as favorable thermodynamically for gylcerides compared to carboxylic acids.

DISCUSSION

The most widely studied OFM molecule both from an experimental and modeling perspective is SA which, in common with HA, has a carboxylic acid headgroup with a saturated aliphatic tailgroup. The only difference is the longer tailgroup for SA (C_{18}) compared to HA (C_6). The present DFT calculations show that HA chemisorbs on α-Fe_2O_3(0001), mostly in its deprotonated state, forming an O−Fe bond through the carbonyl O atom and a H-bond with the surface hydroxyl through the acid O atom. Metastable intact structures were also observed at low coverage, which are slightly less stable than the dissociated ones. These DFT results are in agreement with previous XPS and PM-IRRAS experiments for SA which suggested that chemisorption on steel surfaces occurred through both intact carboxylic acids and dissociated carboxylates.[17] Conversely, TB/MD simulations of SA adsorption on hematite suggested that adsorption occurred through the carboxylic acid and not the carboxylate.[17] Further TB/MD simulations also suggested that SA only chemisorbed on hematite at high surface coverage (3.7 nm^{-2}), with weaker physisorption being more prevalent at low coverage (2.4 nm^{-2}).[34] However, the present DFT calculations suggest that low coverage HA films are also chemisorbed and in fact the adsorption energy for the two coverages considered here (1−4 nm^{-2}) are similar. Since the DFT calculations were performed at 0 K, it is noteworthy that the adsorption energy was shown to be independent of temperature in the TB/MD simulations,[34] suggesting that the observed differences originate from the simulation techniques employed rather than the conditions.

The TB/MD method used in these previous studies[17,34] enables the simulation of relatively large systems dynamically. However, TB requires more approximations regarding the treatment of the electronic structure[32] than the presently employed DFT and does not accurately represent vdW forces.[34] Moreover, it was not directly applied to the system, but it was used to periodically update a classical interatomic potential. Thus, tailgroup-surface interactions are likely to be underestimated in the TB/MD simulations compared to DFT employing a vdW functional[39] and experiment. This means that the adsorption energy is likely to be underestimated, particularly at low coverage, where the tailgroups lie almost flat to the surface. This probably accounts for the observed differences in adsorption behavior between TB/MD and DFT. Thus, the present study demonstrates that an accurate description of the electronic structure, including vdW forces, is very important to study the adsorption behavior of these surfactants. While further studies with ab initio NEMD would surely be beneficial in order to further understand changes in the dynamics of the films with temperature, pressure, and sliding speed, they should be performed with DFT using vdW functionals.[31]

Our calculations have also shown the importance of hydroxylation of the hematite surface. Indeed, the dissociated structures for HA and GMH are stabilized by hydroxylation of the surface via the H atom resulting from the deprotonation. Hematite surfaces in contact with a humid atmosphere tend to naturally hydroxylate to some extent.[67] The role of the hydroxylation in stabilizing deprotonated acid headgroups was also noted in a previous XPS, FTIR and DFT study of the adsorption of sodium laureate in aqueous environments.[68] Sodium laureate does not contain an acidic H to contribute to surface binding, similar to dissociated HA. The most stable structures for sodium laureate on hematite were found to be mediated by the hydroxylated surface sites.[68] However, TB/MD simulations suggested that while SA mostly chemisorbs on iron oxide, it mostly physisorbs on iron hydroxide.[34] Thus, hydroxylation of the surface is expected to significantly affect adsorption behavior of these surfactants. While a complete study of surfactants on hydroxylated hematite is beyond the scope of the present study, this is certainly an important area for future work. It would also be interesting to compare these results to those for adsorption on nascent iron surfaces[34] which can be exposed during rubbing.[31]

The insights provided by this study also help to reconcile friction results from macroscopic tribology experiments and classical NEMD simulations. Several experimental investigations have suggested that monolayer formation on opposing sliding surfaces leads to the low friction and wear observed for OFM-containing lubricants.[4] More recently, NEMD simulations have shown that the formation of OFM monolayers with a high surface coverage are critical to effective friction reduction.[20] In NEMD simulations at a given surface coverage,[20] glycerides gave friction coefficients ∼30% lower

DOI: 10.1021/acs.jpcc.8b05899
J. Phys. Chem. C 2018, 122, 20817−20826

than carboxylic acids. Although glycerides also gave lower friction in macroscopic friction experiments at a given concentration, the difference was only ≤10%.[7] The present DFT study shows that, although glycerides adsorb more strongly onto hematite surfaces compared to carboxylic acids, forming more stable films at all coverages, they have a smaller thermodynamic drive toward the formation of high coverage films. Indeed, while HA molecules show a similar adsorption energy at high coverage compared to low coverage, for GMH closer-packing involves a weaker binding by 0.5−0.9 eV (Figure 4). Collectively, this information suggests that glycerides will form lower coverage films than carboxylic acids in macroscopic friction experiments performed at equal concentration.[7] This postulation could be tested experimentally by comparing carboxylic acid and glyceride film formation on iron oxide surfaces.[12,14] The lower coverage for glycerides compared to acids means that the films are less densely packed, leading to a smaller reduction in friction than might be expected at equal surface coverage. Hence, in the surfactants studied here, there is a trade-off between maximizing adsorption strength and surface coverage, which should be considered in the molecular design of new OFMs.

It should be noted that recent in situ AFM experiments have suggested that the surface coverage of carboxylic acids on mica surfaces increased with increasing tailgroup length (between C_{10-18}).[15] Therefore, the formation of high coverage films is expected to be more energetically favorable for the longer tailgroups employed in commercial OFMs (C_{12-20}) compared to those studied here (C_6).

The increased understanding of the three molecular systems obtained through the present DFT study open several possibilities for further work. In particular, the accurate adsorption energies obtained could be used to parametrize interface force-fields for classical NEMD simulations of HAm, which does not readily dissociate, on hematite surfaces.[69] NEMD simulations of the dissociated carboxylic acids and glycerides confined between hydroxylated iron oxide surfaces would also complement both this and previous studies.[20]

CONCLUSIONS

In this study, density functional theory has been used to study the interaction of three surfactants with an iron oxide surface. Specifically, the adsorption and dissociation behavior of model friction modifier additives (HA, HAm, and GMH) at different surface coverages on α-Fe_2O_3(0001) has been investigated.

Strong chemisorption on the α-Fe_2O_3(0001) surface is observed in all cases considered. Carboxylic acids and glycerides both have a large thermodynamic drive for dissociation, with the adsorption structure being stabilized by the formation of a surface hydroxyl group. Conversely, amides are more stable when they remain intact under all but the most extreme conditions investigated. At all coverages, the glycerides are more strongly adsorbed than the carboxylic acids and amides due to their flexibility and multiple functional groups which can all act as binding sites. However, the large size of the glyceride headgroup means that glycerides are much more stable at low coverage, where the formation of multiple bonds with the surface is possible, than at high coverage. Conversely, carboxylic acids have similar stability at both low coverage and at high coverage, where vdW forces between proximal tailgroups stabilize the adsorption structures.

This study demonstrates how the chemistry and structure of surfactant headgroups can strongly affect their adsorption behavior. It is postulated that this will directly influence the film structure observed experimentally; for example, glycerides will form lower coverage films than carboxylic acids. Previous studies have shown that this, in turn, will influence their macroscopic friction and wear response. Such factors should certainly be considered for the rational molecular design of new surfactants for use as OFMs.

ASSOCIATED CONTENT

Supporting Information

The Supporting Information is available free of charge on the ACS Publications website at DOI: 10.1021/acs.jpcc.8b05899.

Further information regarding the testing of the DFT setup, derivation of the ab initio thermodynamics equations, and additional structural models (PDF)

AUTHOR INFORMATION

Corresponding Author

*E-mail: chiara.gattinoni@mat.ethz.ch.

ORCID

Chiara Gattinoni: 0000-0002-3376-6374

James P. Ewen: 0000-0001-5110-6970

Daniele Dini: 0000-0002-5518-499X

Notes

The authors declare no competing financial interest.

ACKNOWLEDGMENTS

C.G. is supported by the European Unions Horizon 2020 research and innovation programme under the Marie Skłodowska-Curie Grant Agreement No. 744027. J.P.E. acknowledges the financial support of the Engineering and Physical Sciences Research Council (EPSRC) via a Doctoral Prize Fellowship. D.D. also thanks the EPSRC for an Established Career Fellowship EP/N025954/1 and Grant EP/P030211/1. We acknowledge the use of Imperial College London Research Computing Service (RCS). All data reported in the manuscript can be obtained by emailing the corresponding author or tribology@imperial.ac.uk.

REFERENCES

(1) Heinz, H.; Pramanik, C.; Heinz, O.; Ding, Y.; Mishra, R. K.; Marchon, D.; Flatt, R. J.; Estrela-Lopis, I.; Llop, J.; Moya, S.; et al. Nanoparticle decoration with surfactants: molecular interactions, assembly, and applications. *Surf. Sci. Rep.* **2017**, *72*, 1−58.

(2) Araujo, A. C.; Viana, P. R. M.; Peres, A. E. C. Reagents in iron ores flotation. *Miner. Eng.* **2005**, *18*, 219−224.

(3) Zhu, Y.; Free, M. L.; Woollam, R.; Durnie, W. A review of surfactants as corrosion inhibitors and associated modeling. *Prog. Mater. Sci.* **2017**, *90*, 159−223.

(4) Spikes, H. Friction Modifier Additives. *Tribol. Lett.* **2015**, *60*, 5.

(5) Holmberg, K.; Erdemir, A. Influence of tribology on global energy consumption, costs and emissions. *Friction* **2017**, *5*, 263−284.

(6) Simič, R.; Kalin, M. Adsorption mechanisms for fatty acids on DLC and steel studied by AFM and tribological experiments. *Appl. Surf. Sci.* **2013**, *283*, 460−470.

(7) Campen, S.; Green, J.; Lamb, G.; Atkinson, D.; Spikes, H. On the increase in boundary friction with sliding speed. *Tribol. Lett.* **2012**, *48*, 237−248.

(8) Dwivedi, D.; Lepkova, K.; Becker, T. Carbon steel corrosion: A review of key surface properties and characterization methods. *RSC Adv.* **2017**, *7*, 4580−4610.

(9) Jaishankar, A.; Jusufi, A.; Vreeland, J. L.; Deighton, S. P.; Schilowitz, A. Correcting for solvent replacement effects in quartz

crystal microbalance measurements. *Sens. Actuators, A* **2018**, *277*, 60−64.
(10) Watanabe, S.; Nakano, M.; Miyake, K.; Sasaki, S. Analysis of the interfacial molecular behavior of a lubrication film of n-dodecane containing stearic acid under lubricating conditions by sum frequency generation spectroscopy. *Langmuir* **2016**, *32*, 13649−13656.
(11) Campana, M.; Teichert, A.; Clarke, S.; Steitz, R.; Webster, J. R. P.; Zarbakhsh, A. Surfactant adsorption at the metal-oil interface. *Langmuir* **2011**, *27*, 6085−6090.
(12) Wood, M. H.; Casford, M. T.; Steitz, R.; Zarbakhsh, A.; Welbourn, R. J. L.; Clarke, S. M. Comparative adsorption of saturated and unsaturated fatty acids at the iron oxide/oil interface. *Langmuir* **2016**, *32*, 534−540.
(13) Ruths, M.; Lundgren, S.; Danerlov, K.; Persson, K. Friction of fatty acids in nanometer-sized contacts of different adhesive strength. *Langmuir* **2008**, *24*, 1509−1516.
(14) Campen, S.; Green, J. H.; Lamb, G. D.; Spikes, H. A. In situ study of model organic friction modifiers using liquid cell AFM; saturated and mono-unsaturated carboxylic acids. *Tribol. Lett.* **2015**, *57*, 18.
(15) Bernat, S.; Armada, S.; Espallargas, N. Friction mechanisms by carboxylic acids in aqueous lubricants. *Tribol. Lett.* **2018**, *66*, 83.
(16) Sahoo, R. R.; Biswas, S. K. Frictional response of fatty acids on steel. *J. Colloid Interface Sci.* **2009**, *333*, 707−718.
(17) Loehlé, S.; Matta, C.; Minfray, C.; Le Mogne, T.; Iovine, R.; Obara, Y.; Miyamoto, A.; Martin, J.-M. Mixed lubrication of steel by C18 fatty acids revisited. Part I: toward the formation of carboxylate. *Tribol. Int.* **2015**, *82*, 218−227.
(18) Ewen, J. P.; Heyes, D. M.; Dini, D. Advances in nonequilibrium molecular dynamics simulations of lubricants and additives. *Friction* **2018**, DOI: 10.1007/s40544-018-0207-9.
(19) Doig, M.; Warrens, C. P.; Camp, P. J. Structure and friction of stearic acid and oleic acid films adsorbed on iron oxide surfaces in squalane. *Langmuir* **2014**, *30*, 186−195.
(20) Ewen, J. P.; Gattinoni, C.; Morgan, N.; Spikes, H. A.; Dini, D. Nonequilibrium molecular dynamics simulations of organic friction modifiers adsorbed on iron oxide surfaces. *Langmuir* **2016**, *32*, 4450−4463.
(21) Ewen, J. P.; Kannam, S. K.; Todd, B. D.; Dini, D. Slip of alkanes confined between surfactant monolayers adsorbed on solid surfaces. *Langmuir* **2018**, *34*, 3864−3873.
(22) Bradley-Shaw, J. L.; Camp, P. J.; Dowding, P. J.; Lewtas, K. Self-assembly and friction of glycerol monooleate and its hydrolysis products in bulk and confined non-aqueous solvents. *Phys. Chem. Chem. Phys.* **2018**, *20*, 17648−17657.
(23) Jones, R. O. Density functional theory: its origins, rise to prominence, and future. *Rev. Mod. Phys.* **2015**, *87*, 897−923.
(24) Shenghua, L.; He, Y.; Yuansheng, J. Lubrication chemistry viewed from DFT-based concepts and electronic structural principles. *Int. J. Mol. Sci.* **2004**, *5*, 13−34.
(25) Kokalj, A.; Peljhan, S.; Fingar, M.; Miloev, I. What determines the inhibition effectiveness of ATA, BTAH, and BTAOH corrosion inhibitors on copper? *J. Am. Chem. Soc.* **2010**, *132*, 16657−16668.
(26) Gattinoni, C.; Michaelides, A. Understanding corrosion inhibition with van der Waals DFT methods: The case of benzotriazole. *Faraday Discuss.* **2015**, *180*, 439−458.
(27) Hernández Velázquez, J. D.; Barroso-Flores, J.; Gama Goicochea, A. *Ab initio* modeling of friction reducing agents shows quantum mechanical interactions can have macroscopic manifestation. *J. Phys. Chem. A* **2016**, *120*, 9244−9248.
(28) Righi, M. C.; Loehlé, S.; De Barros Bouchet, M. I.; Mambingo-Doumbe, S.; Martin, J.-M. A comparative study on the functionality of S- and P-based lubricant additives by combined first principles and experimental analysis. *RSC Adv.* **2016**, *6*, 47753−47760.
(29) Loehlé, S.; Righi, M. C. First principles study of organo-phosphorus additives in boundary lubrication conditions: Effects of hydrocarbon chain length. *Lubr. Sci.* **2017**, *29*, 485−491.
(30) Osei-Agyemang, E.; Berkebile, S.; Martini, A. Decomposition mechanisms of anti-wear lubricant additive tricresyl phosphate on iron surfaces using DFT and atomistic thermodynamic studies. *Tribol. Lett.* **2018**, *66*, 48.
(31) Loehlé, S.; Righi, M. C. *Ab initio* molecular dynamics simulation of tribochemical reactions involving phosphorus additives at sliding iron interfaces. *Lubricants* **2018**, *6*, 31.
(32) Sutton, A. P.; Finnis, M. W.; Pettifor, D. G.; Ohta, Y. The tight-binding bond model. *J. Phys. C: Solid State Phys.* **1988**, *21*, 35−66.
(33) Loehlé, S.; Matta, C.; Minfray, C.; Le Mogne, T.; Martin, J.-M.; Iovine, R.; Obara, Y.; Miura, R.; Miyamoto, A. Mixed lubrication with C18 fatty acids: effect of unsaturation. *Tribol. Lett.* **2014**, *53*, 319−328.
(34) Loehlé, S.; Matta, C.; Minfray, C.; Le Mogne, T.; Iovine, R.; Obara, Y.; Miyamoto, A.; Martin, J.-M. Mixed lubrication of steel by C18 fatty acids revisited. Part II: Influence of some key parameters. *Tribol. Int.* **2016**, *94*, 207−216.
(35) Kresse, G.; Hafner, J. *Ab initio* molecular dynamics for liquid metals. *Phys. Rev. B: Condens. Matter Mater. Phys.* **1993**, *47*, 558−561.
(36) Kresse, G.; Furthmuller, J. Efficiency of ab-initio total energy calculations for metals and semiconductors using a plane-wave basis set. *Comput. Mater. Sci.* **1996**, *6*, 15−50.
(37) Kresse, G.; Furthmuller, J. Efficient iterative schemes for *ab initio* total-energy calculations using a plane-wave basis set. *Phys. Rev. B: Condens. Matter Mater. Phys.* **1996**, *54*, 11169−11186.
(38) Kresse, G.; Joubert, D. From ultrasoft pseudopotentials to the projector augmented-wave method. *Phys. Rev. B: Condens. Matter Mater. Phys.* **1999**, *59*, 1758−1775.
(39) Klimeš, J.; Bowler, D. R.; Michaelides, A. Van der Waals density functionals applied to solids. *Phys. Rev. B: Condens. Matter Mater. Phys.* **2011**, *83*, 195131.
(40) Lew, W.; Crowe, M. C.; Campbell, C. T.; Carrasco, J.; Michaelides, A. The energy of hydroxyl coadsorbed with water on Pt(111). *J. Phys. Chem. C* **2011**, *115*, 23008−23012.
(41) Liu, W.; Carrasco, J.; Santra, B.; Michaelides, A.; Scheffler, M.; Tkatchenko, A. Benzene adsorbed on metals: Concerted effect of covalency and van der Waals bonding. *Phys. Rev. B: Condens. Matter Mater. Phys.* **2012**, *86*, 245405.
(42) Murphy, C. J.; Carrasco, J.; Lawton, T. J.; Liriano, M. L.; Baber, A. E.; Lewis, E. A.; Michaelides, A.; Sykes, E. C. H. Structure and energetics of hydrogen-bonded networks of methanol on close packed transition metal surfaces. *J. Chem. Phys.* **2014**, *141*, 014701.
(43) Carrasco, J.; Liu, W.; Michaelides, A.; Tkatchenko, A. Insight into the description of van der Waals forces for benzene adsorption on transition metal (111) surfaces. *J. Chem. Phys.* **2014**, *140*, 084704.
(44) Bedolla, P. O.; Feldbauer, G.; Wolloch, M.; Eder, S. J.; Dorr, N.; Mohn, P.; Redinger, J.; Vernes, A. Effects of van der Waals Interactions in the Adsorption of Isooctane and Ethanol on Fe(100) Surfaces. *J. Phys. Chem. C* **2014**, *118*, 17608−17615.
(45) Liriano, M. L.; Gattinoni, C.; Lewis, E. A.; Murphy, C. J.; Sykes, E. C. H.; Michaelides, A. Water-ice analogues of polycyclic aromatic hydrocarbons: water nanoclusters on Cu(111). *J. Am. Chem. Soc.* **2017**, *139*, 6403−6410.
(46) Neugebauer, J.; Scheffler, M. Adsorbate-substrate and adsorbate-adsorbate interactions of Na and K adlayers on Al(111). *Phys. Rev. B: Condens. Matter Mater. Phys.* **1992**, *46*, 16067−16080.
(47) Makov, G.; Payne, M. Periodic boundary conditions in *ab initio* calculations. *Phys. Rev. B: Condens. Matter Mater. Phys.* **1995**, *51*, 4014−4022.
(48) Rayne, S.; Forest, K. Theoretical studies on the pKa values of perfluoroalkyl carboxylic acids. *J. Mol. Struct.: THEOCHEM* **2010**, *949*, 60−69.
(49) Tsuzuki, S.; Honda, K.; Uchimaru, T.; Mikami, M. Magnitude of interaction between n-alkane chains and its anisotropy: high-level *ab initio* calculations of n-butane, n-pentane, and n-hexane dimers. *J. Phys. Chem. A* **2004**, *108*, 10311−10316.
(50) Tsuzuki, S.; Honda, K.; Uchimaru, T.; Mikami, M. Estimated MP2 and CCSD(T) interaction energies of n-alkane dimers at the basis set limit: Comparison of the methods of Helgaker *et al.* and Feller. *J. Chem. Phys.* **2006**, *124*, 114304.

DOI: 10.1021/acs.jpcc.8b05899
J. Phys. Chem. C 2018, 122, 20817−20826

(51) Rojas, L.; Ruette, F.; Peraza, A.; Castellano, O.; Soscún, H. Relationship between unbranched alkane dimer interaction energies using different theoretical methods and correlations with thermodynamic properties. *Chem. Phys. Lett.* **2015**, *625*, 20−25.
(52) Parkinson, G. S. Iron oxide surfaces. *Surf. Sci. Rep.* **2016**, *71*, 272−365.
(53) Dudarev, S. L.; Botton, G. A.; Savrasov, S. Y.; Humphreys, C. J.; Sutton, A. P. Electron-energy-loss spectra and the structural stability of nickel oxide: An LSDA+U study. *Phys. Rev. B: Condens. Matter Mater. Phys.* **1998**, *57*, 1505−1509.
(54) Huang, X.; Ramadugu, S. K.; Mason, S. E. Surface-specific DFT + U approach applied to α-Fe_2O_3(0001). *J. Phys. Chem. C* **2016**, *120*, 4919−4930.
(55) Merchant, P.; Collins, R.; Kershaw, R.; Dwight, K.; Wold, A. The electrical, optical and photoconducting properties of $Fe_{2x}Cr_xO_3$ ($0 \leq x\ 0 \leq .47$). *J. Solid State Chem.* **1979**, *27*, 307−315.
(56) Finger, L. W.; Hazen, R. M. Crystal structure and isothermal compression of Fe_2O_3, Cr_2O_3, and V_2O_3 to 50 kbars. *J. Appl. Phys.* **1980**, *51*, 5362−5367.
(57) Coey, J. M. D.; Sawatzky, G. A. A study of hyperfine interactions in the system $(Fe_{1-x}Rh_x)_2O_3$ using the Mossbauer effect (bonding parameters). *J. Phys. C: Solid State Phys.* **1971**, *4*, 2386.
(58) Krén, E.; Szabó, P.; Konczos, G. Neutron diffraction studies on the (1-x)Fe_2O_3 - xRh_2O_3 system. *Phys. Lett.* **1965**, *19*, 103−104.
(59) Wang, X.-G.; Weiss, W.; Shaikhutdinov, S. K.; Ritter, M.; Petersen, M.; Wagner, F.; Schlögl, R.; Scheffler, M. The hematite (α-Fe_2O_3) (0001) surface: evidence for domains of distinct chemistry. *Phys. Rev. Lett.* **1998**, *81*, 1038−1041.
(60) Liao, P.; Carter, E. A. Testing variations of the GW approximation on strongly correlated transition metal oxides: hematite (α-Fe2O3) as a benchmark. *Phys. Chem. Chem. Phys.* **2011**, *13*, 15189−15199.
(61) Rollmann, G.; Rohrbach, A.; Entel, P.; Hafner, J. First-principles calculation of the structure and magnetic phases of hematite. *Phys. Rev. B: Condens. Matter Mater. Phys.* **2004**, *69*, 165107.
(62) Trainor, T. P.; Chaka, A. M.; Eng, P. J.; Newville, M.; Waychunas, G. A.; Catalano, J. G.; Brown, G. E. Structure and reactivity of the hydrated hematite (0001) surface. *Surf. Sci.* **2004**, *573*, 204−224.
(63) Guo, H.; Barnard, A. S. Thermodynamic modelling of nanomorphologies of hematite and goethite. *J. Mater. Chem.* **2011**, *21*, 11566−11577.
(64) Reuter, K.; Scheffler, M. Composition, structure, and stability of RuO_2(110) as a function of oxygen pressure. *Phys. Rev. B: Condens. Matter Mater. Phys.* **2001**, *65*, 035406.
(65) Lozovoi, A. T.; Alavi, A.; Finnis, M. W. Surface energy and the early stages of oxidation of NiAl(110). *Comput. Phys. Commun.* **2001**, *137*, 174−194.
(66) Bergermayer, W.; Schweiger, H.; Wimmer, E. *Ab initio* thermodynamics of oxide surfaces: O_2on.Fe_2O_3(0001). *Phys. Rev. B: Condens. Matter Mater. Phys.* **2004**, *69*, 195409.
(67) Guo, H.; Barnard, A. S. Surface structure and environment-dependent hydroxylation of the nonpolar hematite (100) from density functional theory modeling. *J. Phys. Chem. C* **2011**, *115*, 23023−23029.
(68) Chernyshova, I. V.; Ponnurangam, S.; Somasundaran, P. Adsorption of Fatty Acids on Iron (Hydr)oxides from Aqueous Solutions. *Langmuir* **2011**, *27*, 10007.
(69) Tromp, S.; Joly, L.; Cobian, M.; Fillot, N. Chemical physics at interfaces within a refrigerant-lubricated contact: from electronic structure to large scale molecular dynamics simulations. *J. Phys. Chem. C* **2018**, *122*, 5420−5429.

DOI: 10.1021/acs.jpcc.8b05899
J. Phys. Chem. C 2018, 122, 20817−20826